Research Article

Feng Wang*, Fengshou Zhang, Jiang Ma, and Xizhen Ma

Technology and analysis of 08Cr9W3Co3VNbCuBN steel large diameter thick wall pipe welding process

https://doi.org/10.1515/htmp-2022-0256 received June 09, 2022; accepted November 16, 2022

Abstract: In this article, the welding technology of large diameter thick wall 08Cr9W3Co3VNbCuBN (G115) heatresistant steel pipes for the main steam pipe of a 650°C ultra-supercritical power station boiler has been investigated, and the mechanical properties and microstructure of welded joints at different wall thickness positions have also been analyzed. The results show that the mechanical properties of narrow gap welded joint of 115 mm thick large diameter 08Cr9W3Co3VNbCuBN heat-resistant steel pipe obtained by Gas tungsten arc welding (GTAW) + shielded metal arc welding (SMAW) + automatic submerged arc welding (SAW) can meet the requirements of relevant standards after tempering at 780°C. The tensile failure of the welded joint occurs in the base metal zone far away from the weld, an obvious necking phenomenon appears at the fracture position, and the welded joint has good tensile properties. No δ ferrite phase was found in the weld and heat-affected zone (HAZ). The microstructures of each zone are tempered martensite.

Keywords: ultra supercritical power plant boiler, large diameter thick wall pipe, 08Cr9W3Co3VNbCuBN heatresistant steel, wedding technology, mechanical properties

1 Introduction

With the development of economy and society, energy saving and emission reduction have become the two major

* Corresponding author: Feng Wang, Research and Management Department, The Boiler & Pressure Vessel Safety Inspection Institute of Henan Province, Zhengzhou, Henan 450016, PR China, e-mail: 5096219@qq.com, tel: +86 18137775980 Fengshou Zhang: General Engineer Office, Henan Huadian Jinyuan Piping Co., Ltd., Zhengzhou, Henan, 451162, PR China Jiang Ma, Xizhen Ma: Research and Management Department,

The Boiler & Pressure Vessel Safety Inspection Institute of Henan Province, Zhengzhou, Henan 450016, PR China

themes in the development of the modern industry. Ultrasupercritical thermal power unit technology with high energy efficiency and low emission has gradually become the development direction of thermal power unit technology.

In 2017, the National Energy Administration of China officially approved the demonstration project of Da tang Yuncheng 630°C ultra-supercritical coal-fired unit, which is currently the thermal power unit with the highest steam parameters in the world. The efficiency of thermal power units depends mainly on the steam temperature and steam pressure of the units, and the efficiency of the generating units can be effectively improved only by increasing the steam parameters. To achieve reliable operation of units with higher steam parameters, it is necessary to research and develop high-temperature heat-resistant materials that are compatible with high steam parameters. But for now, the development of heat-resistant steel in high-temperature sections is the key factor restricting the development of thermal power units to high parameters, and the large diameter thick wall boiler tube is the bottleneck [1–3].

A new type of martensitic heat-resistant steel 08Cr9W3Co3VNbCuBN (G115) was jointly developed by the Iron and Steel Research Institute and Bao Steel group. The steel adopts selective strengthening to effectively control the growth rate of M₂₃C₆ carbides during service by reasonably controlling the ratio of B to N, adding an appropriate amount of Cu further increases the precipitation strengthening effect. The durable extrapolated strength at 650°C for 10,000 h is 1.5 times that of P92 steel, and its resistance to high-temperature steam oxidation and welding ability is equivalent to that of P92 steel [4]. At present, the research on 08Cr9W3Co3VNbCuBN steel is limited to the manufacturing process and performance of 08Cr9W3Co3VNb-CuBN steel base metal and small diameter superheater and reheater tube [5-8], while the welding technology research of large diameter thick wall 08Cr9W3Co3VNbCuBN steel is rarely reported.

08Cr9W3Co3VNbCuBN steel belongs to the 9% Cr family of heat-resistant steels, and Kumar et al. [9,10] found the presence of δ ferrite with different morphologies in

the coarse-grained HAZ (CGHAZ) region of welded joints of 9% Cr family heat-resistant steels [9–12], and the presence of δ ferrite significantly reduces the impact toughness of welded joints and has a negative impact on the long-term creep strength of welded joints [13].

08Cr9W3Co3VNbCuBN steel contains about 3% Co, 0.8% Cu elements, both of which are austenite stabilizing elements that can inhibit the formation of δ ferrite, but during the performance heat treatment of large diameter thick wall heat-resistant steel pipe, due to the wall thickness and long heating and holding time, there is an obvious temperature gradient at different positions in the pipe diameter direction during cooling, which usually leads to the coarser grain size of the base metal. When welding coarse-grained thick wall 08Cr9W3Co3VNbCuBN steel, if the welding process is not selected properly, micro defects such as δ ferrite phase and carbide precipitation growth along the crystal are easy to appear at the welded joint, which will adversely affect its mechanical properties, especially the impact properties.

In this article, the welding process of 08Cr9W3Co3VNbCuBN heat-resistant pipe with a wall thickness of 115 mm, which can be used for the main steam pipe of 650°C power station boiler, was studied. The mechanical properties and microstructure of narrow gap welded joints of 08Cr9W3Co3VNbCuBN steel pipe at different wall-thickness positions have been detected and analyzed.

2 Experimental procedures

2.1 Materials

The test material is 08Cr9W3Co3VNbCuBN (G115) heat-resistant steel pipe for 650°C power station boiler, with the size of outer diameter 530 mm × 115 mm. The chemical composition of 08Cr9W3Co3VNbCuBN steel pipe is shown in Table 1. According to Table 1, the chemical composition of 08Cr9W3Co3VNbCuBN steel pipe meets the relevant requirements of the group standard T/CISA 003-2017 new martensitic heat-resistant steel 08Cr9W3Co3VNbCuBN seamless steel pipe for power station. The microstructure of 08Cr9W3Co3VNbCuBN steel is typical tempered martensite, as shown in Figure 1.

2.2 Welding and post-weld heat treatment process

GTAW, SMAW and SAW methods are used for thick-walled 08Cr9W3Co3VNbCuBN steel pipe. Jing lei GTR-

Table 1: Chemical composition of the 08Cr9W3Co3VNbCuBN pipe and welding stick (mass fraction, %)

Element	U	Mn	Si	Si Cr W	×	>	ဝ	z	B	Cu Nb		ΑI	S	Al S P Fe
Standard value of	0.06-0.10	0.06-0.10 0.27-0.73	≤0.5	8.5-9.5	2.33-3.17	0.13-0.27	2.85-3.25	≤0.5 8.5-9.5 2.33-3.17 0.13-0.27 2.85-3.25 0.005-0.015 0.01-0.022 0.4-1.2 0.03-0.1 ≤0.015 ≤0.01 ≤0.02 Bal	0.01-0.022	0.4 - 1.2	0.03-0.1	<0.015	<0.01	<0.02 B
08Cr9W3Co3VNbCuBN steel [14]														
Measured value of	0.08	0.40	0.17	0.17 8.74 2.7	2.7	0.253	2.85	0.012	0.016	0.62 0.06		0.004	0.005	0.004 0.005 0.017 Bal
08Cr9W3Co3VNbCuBN steel pipe														
GTR-W93 welding wire	0.10	09.0	0.36 8.82	8.82	2.31	0.19	2.82	ı	ı	0.01	ı	1	0.004	0.009 B
GER-93 welding wire	0.07	0.72	0.13	9.00	2.75	0.17	2.72	ı	I	0.83	ı	ı	0.004	0.004 0.006 Bal
GWR-W93 welding wire	0.11	0.77	0.11	8.52	2.68	0.20	2.89	ı	ı	0.08	ı	ı	0.005	0.006 B

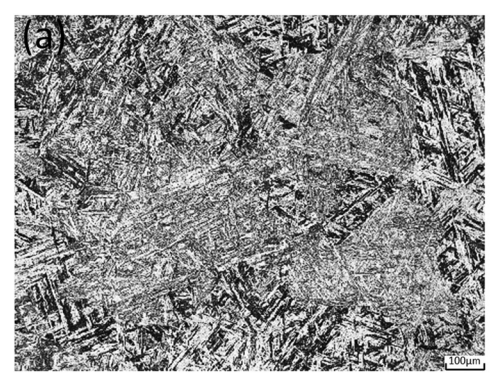




Figure 1: Microstructure of 08Cr9W3Co3VNbCuBN steel. (a) 100X, (b) 500X.

W93 wire electrode with a diameter of Ø2.4 mm was utilized for GTAW, GER-93 welding rod with a diameter of Ø3.2 mm was utilized for SMAW, and GWR-W93 wire electrode with the GXR-93 welding flux was utilized in the SAW process. The chemical composition and mechanical properties of the welding rod (wire) are shown in Tables 1 and 2.

The welding groove of thick-walled 08Cr9W3Co3VNbCuBN steel pipe adopts a double V-shaped narrow gap groove, and the butt width is 31-32 mm. The specific parameters are shown in Figure 2. After the pipe butt joint inspection is qualified, the steel pipe is pre-heated at $200-250^{\circ}$ C for 1.5 h. The spot welding is carried out, applying the Ø2.4 mm tungsten electrode, grade WCE-20 (tip sharpening angle, $20-30^{\circ}$) under the DC + polarity.

The protruding length of the tungsten electrode from the porcelain nozzle is less than or equal to 8 mm, and the arc length between the tungsten electrode and the surface of the molten pool is 2-4 mm. Two weld passes with a thickness of 3 mm each are made by GTAW. During the first layer of argon arc welding and manual welding, the pipeline should be filled with argon for protection, and the purity of argon used should be greater than 99.9%. The flow of internal shielding gas is $0.37-0.5 \, \text{L·s}^{-1}$ at the beginning and $0.15-0.23 \, \text{L·s}^{-1}$ during welding.

There are 46 welding layers in total: the first and second layers are GTAW primer, the 3rd-14th layers are made by SMAW, and the 15th-46th layers are made by SAW. The 3rd, 4th and 5th layers are single-layer single pass welding, the 6th-39th layers are welded with two passes per layer, the 40th-44th are welded with three passes per layer, and the 45th-46th layers are welded with four passes per layer. Table 3 lists specific welding process parameters.

During preheating and heat tracing, thermocouples are placed on both sides of the groove, the temperature at the digital display is recorded every 30 min, and the temperature at the edge of the groove is measured and recorded by a contact thermometer. In the process of GTAW and SMAW welding, the interlayer temperature is always maintained in the range of 200–250°C, and in the process of submerged arc welding, the interlayer temperature is always maintained in the range of 200–300°C.

The initial temperature of the martensitic transformation of 08Cr9W3Co3VNbCuBN steel is 375°C, and the completion temperature of martensitic transformation is 255°C [15]. After welding, the temperature is kept at 255°C for 2 h to complete the martensitic transformation, and then, the

Table 2: Mechanical properties of the 08Cr9W3Co3VNbCuBN pipe and welding electrodes

Mechanical properties of elements	Tensile strength (MPa)	Yield strength (MPa)	Elongation, % (portrait)	KV ₂ /J (portrait)	Hardness/HBW
Standard value of 08Cr9W3Co3VNbCuBN steel [14]	≥660	≥480	≥20	≥40	195–250
Measured value of 08Cr9W3Co3VNbCuBN steel pipe	675	526	27	121	219
GTR-W93 welding wire	781	654	22	96	_
GER-W93 welding rod	729	596	20	108	_
GWR-W93 welding wire	735	580	25	44	_

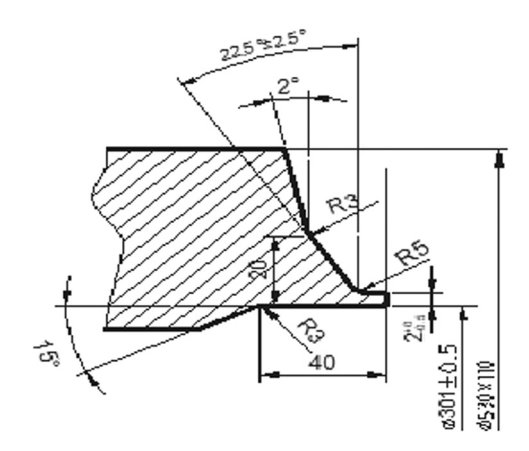


Figure 2: Schematic diagram of welding groove of thick wall 08Cr9W3Co3VNbCuBN steel pipe.

temperature is increased to 350°C, kept constant for 2h and cooled slowly.

The overall heat treatment in the furnace is adopted in the post-weld heat treatment. The constant temperature is 775 \pm 5°C, the constant temperature time is 11 h, the heating rate is less than 60 K·h⁻¹, the cooling rate is less than 90 K·h⁻¹, and the temperature is decreased to below 300°C by air cooling.

2.3 Sampling location and testing method

After the completion of welding heat treatment, the welded joint is qualified by ultrasonic and X-ray non-destructive testing. With the weld seam as the center along the longitudinal direction of the pipe, the workpiece is cut into eight pieces by wire cutting and numbered 1–8, geometry and dimensions of the corresponding test block as shown in Figure 3a. Six tensile specimens were wire cut out of block No. 1. Four side bending specimens were cut of block No. 8. Eighteen impact specimens were cut out of block No. 3, including nine welding impact specimens and nine HAZ

impact specimens. The metallographic sampling position is shown in Figure 3b.

After grinding and polishing, the metallographic samples are corroded with FeCl₃ hydrochloric acid solution (5 g ferric chloride, 50 mL hydrochloric acid and 100 mL water) and observed under Axio A1m Zeiss optical microscope. The room temperature tensile test was carried out on CMT5105 Mets tensile testing machine according to GB/ T228.1-2010. The impact test of welded joints was carried out at room temperature according to GB/T 229-2007 on ZBC2302-C Mets impact testing machine. The notch axis of the HAZ sample passes through the fusion line and is perpendicular to the weld surface, and the notch axis of the weld sample is located in center of the weld and perpendicular to the weld surface. HV-30T Vickers hardness tester is used to test the hardness of different areas of the welded joint profile according to GB/T 9790-2021. Vickers hardness measurement load is 9.8 N. From the fusion line on both sides of the weld, the hardness testing points of HAZ are tested every 0.5 mm.

3 Results and discussion

3.1 Microstructure of welded joints

As shown in Figure 3b, the metallographic samples of base metal, HAZ and weld at different thickness positions of No. 1–3 welded joints section are observed and analyzed. The metallographic morphology of the base metal at different section thickness positions of No. 1–3 welded joints section is shown in Figure $4a_1$ – a_3 , where the microstructure is tempered martensite and basically consistent with the metallographic morphology of the raw material of 08Cr9W3Co3VNbCuBN steel pipe shown in Figure 1.

Figure 4b₁-b₃ shows the metallographic morphology of the HAZ at different locations, where the microstructure

Table 3: Welding parameter

Welding mode	Welding layer	Welding technology	Weldi	ng wire	Welding current (A)	Arc voltage (V)	Wire feeding speed (cm·min ⁻¹)	Welding speed (cm·min ⁻¹)
			Diameter (mm)	Brand				
Backing welding	1–2	GTAW	2.4	GTR-W93	110-160	10-15	_	3–10
Filler welding	3-14	SMAW	3.2	GER-W93	90-135	22-25	_	14-51
Filler welding + cover welding	15–46	SAW	2.4	GWR-W93	300-380	28-35	686-857.5	26–46





Figure 3: Schematic diagram of sampling position.

is still tempered martensite, but the grain size of the original austenite is significantly finer than that of the base metal. The width of HAZ of narrow gap welded joint of thick-walled 08Cr9W3Co3VNbCuBN steel pipe obtained by GTAW, SMAW and SAW is 2–3 mm, which can be divided into four parts: fusion zone, coarse grain zone, fine grain zone and incomplete recrystallization zone. However, there

is no obvious difference in grain morphology in different positions of HAZ of thick-walled 08Cr9W3Co3VNbCuBN steel pipe, which is finer than that of the base metal. In addition, we have marked the relevant grain boundaries with red curves in the figure.

Figure $4c_1$ – c_3 shows the metallographic morphology of the weld at different positions; the microstructure is laid of tempered martensite, which consists of a large number of equiaxed crystals and small amounts of columnar crystals. The reason for the smaller amounts of columnar crystals is that the 46 passes of the welded joint are reheated by the subsequent weld bead at the sampling position, resulting in phase transformation and recrystallization of the microstructure at the sampling position, forming a large number of equiaxed crystals.

Both thick-walled 08Cr9W3Co3VNbCuBN base metal and welding metal contain about 9 wt.% Cr and 2.7wt.% W. The results show that too high Cr and W content will lead to the emergence of δ -Fe [16,17], but the Co and Cu elements in 08Cr9W3Co3VNbCuBN steel are austenite stabilizing elements, which can effectively restrain the

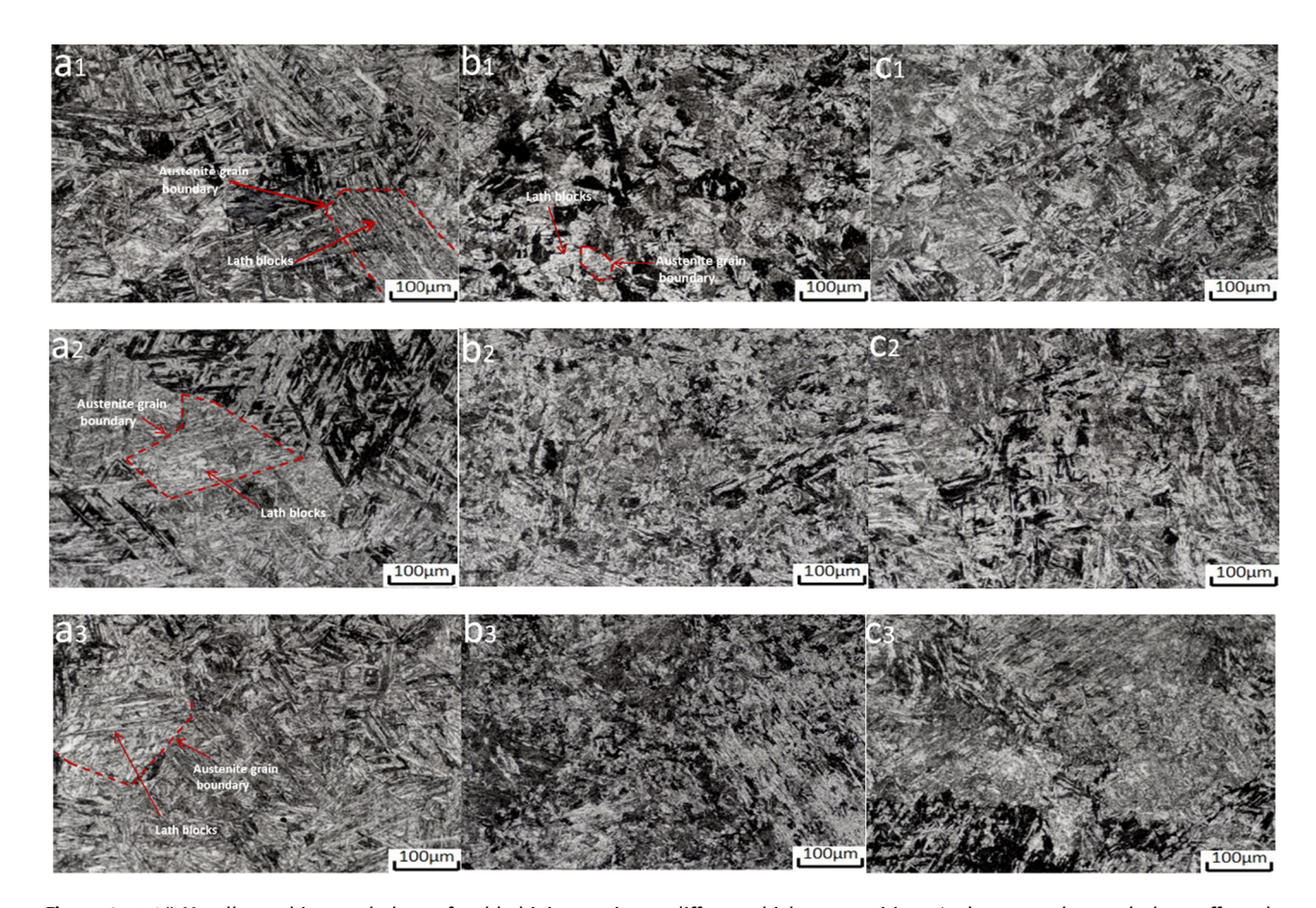


Figure 4: 1–3# Metallographic morphology of welded joint section at different thickness positions (a, base metal zone; b, heat affected zone; c, weld zone).

emergence of δ -Fe. The microstructure of all parts of the welded joint of 08Cr9W3Co3VNbCuBN steel obtained by the welding process described in this article is tempered martensite and no δ -Fe is found.

3.2 Tensile and impact properties of welded joints

As shown in Figure 3a, the No. 1 specimen is stretched at room temperature. The tensile strength of the welded joint is $665-695\,\mathrm{MPa}$; the test meets the requirements of tensile $(R_\mathrm{m}) \ge 660\,\mathrm{MPa}$ of steel pipe in TCISA 003-2017 standard. The tensile failure of the welded joint occurs in the base metal area away from the weld, and the obvious necking phenomenon appears at the fracture position; welded joint tensile specimen fracture location is shown in Figure 5.

No. 8 specimen is subjected to side bending. In accordance with the requirements of TCISA 003-2017 standard in D=4a, $\alpha=180^{\circ}$ bending conditions of the inside and outside surface of the side bending specimens are not seen cracks, to meet the standard requirements.

No. 3 specimen is tested by room temperature impact test according to the different thickness positions of the welded joint section No. 1–3 as shown in Figure 3b. As shown in Figure 6, the impact energy of weld zone of the No. 1–3 welded joint section (as Figure 3b cross section) is 73, 62 and 84 J, respectively, and that of HAZ is 52, 61 and 79 J, respectively.

The change pattern of impact performance at different thickness positions is basically the same. The impact energy of the HAZ of the welded joint obtained

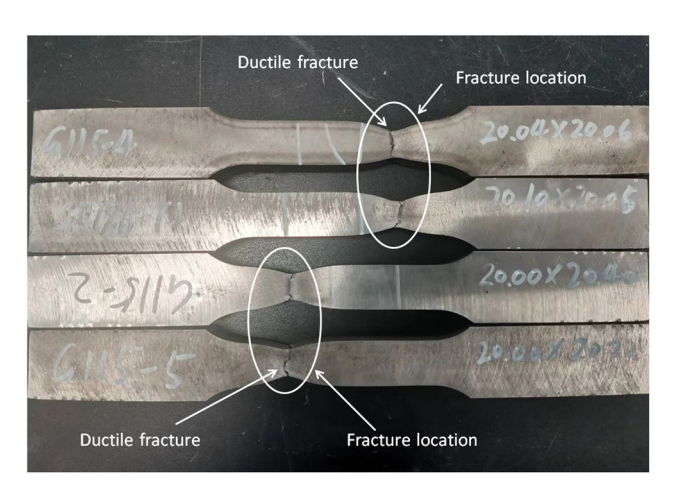


Figure 5: Welded joint tensile specimen fracture location.

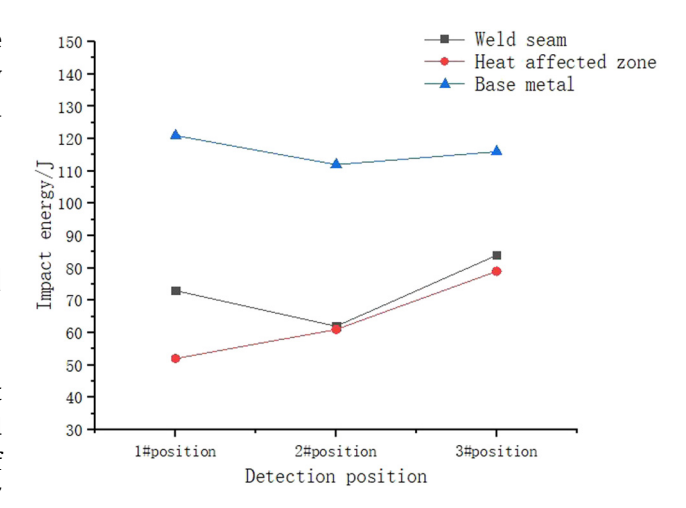


Figure 6: 1–3# Impact energy of weld seam and heat affected zone of welded joint section.

by GTAW + SMAW + SAW process is the lowest, the impact energy of the weld position is only 52 J, and the impact property of the weld zone is slightly better than that of the HAZ (the lowest 62 J), but also obviously lower than that of the base metal (average 120 J). The impact energy of each region meets the impact performance requirements of steel pipes in the TCISA003-2017 standard (longitudinal impact energy \geq 40 J).

3.3 Vickers hardness of welded joints

As shown in Figure 7, the hardness of the welded joint of No. 1–3 shared the same hardness variation law, the hardness of HAZ is significantly higher than that of

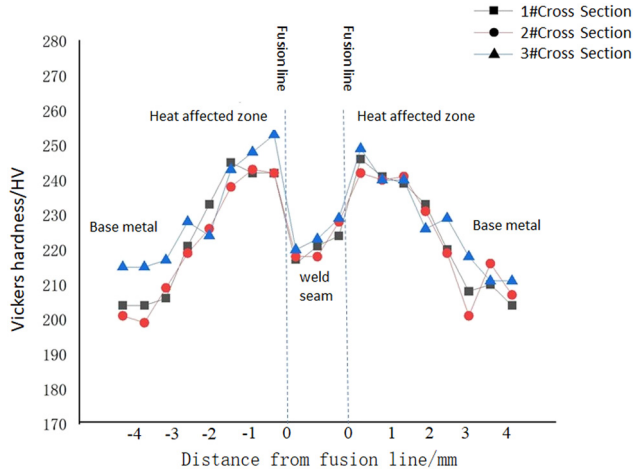


Figure 7: 1–3# Vickers hardness in different areas of Welded joint section.

base metal and weld zone, and the Vickers hardness near the fusion line of HAZ in the section of No. 3 reaches 253 HV. As the measuring point is far away from the weld, its hardness test value decreases gradually, and the hardness value is basically the same as the average hardness of the base metal at about 2.5 mm from the weld fusion line. According to the changes of metallographic structure and hardness, it can be determined that the width of HAZ of narrow gap thick wall 08Cr9W3Co3VNbCuBN welded joint obtained by GTAW, SMAW, and SAW is about 2.5 mm.

Generally, the HAZ can be divided into fusion zone, coarse grain zone, fine grain zone and incomplete recrystallization zone. Since the 08Cr9W3Co3VNbCuBN steel pipe with a wall thickness of 115 mm has been welded in 46 layers by the welding process described in this article, the HAZ of 08Cr9W3Co3VNbCuBN steel has experienced many short-term heating and cooling cycles. During the heating process, the HAZ quickly passes through the A_{c1}-A_{c3} critical zone under the action of welding heat, so that the flake austenite cannot grow in time, and the austenite is mainly spherical, and the austenite grain is refined after a single thermal cycle [18]. In the subsequent thermal cycles, there is no fixed orientation relationship between martensite and spherical austenite, and the precipitated MC-type carbides are pinned to the grain boundary, and finally, the microstructure of HAZ with grain refinement is obtained. At the same time, the presence of Co and Cu elements in G115 steel inhibits the formation of δ ferrite in the weld heat-affected zone. Therefore, the hardness of HAZ is 20-30 HV higher than that of base metal.

4 Conclusions

In this article, the welding process of 08Cr9W3Co3VNbCuBN heat-resistant pipe with a wall thickness of 115 mm, which can be used for the main steams pipe of 650°C power station boiler, is studied, and the mechanical properties and microstructure of narrow gap welded joint of thick-walled 08Cr9W3Co3VNbCuBN steel pipe are tested and analyzed.

- (1) The narrow gap welded joint of 115 mm thick large diameter 08Cr9W3Co3VNbCuBN heat-resistant steel pipe obtained by GTAW, SMAW and SAW welding process can meet the requirements of relevant standards.
- (2) The width of HAZ of narrow gap welded joint of 115 mm thick large diameter 08Cr9W3Co3VNbCuBN heat-resistant steel pipe obtained by GTAW, SMAW and SAW is about 2.5 mm, and its hardness up to 253HV is significantly higher than that of the weld and base metal area.

(3) The microstructure of the welded joint of 115 mm thick large diameter 08Cr9W3Co3VNbCuBN steel is tempered martensite, and the grain in the welding HAZ is refined, and no δ -Fe is found in all parts of the welded joint.

Acknowledgments: The authors sincerely acknowledge Gao Mengjie and Professor Zhai Yunpu, School of Chemistry, Zhengzhou University, for their support to this research.

Funding information: The authors state no funding is involved.

Author contributions: Feng Wang - writing-original draft, writing – review & editing, methodology, formal Analysis; Fengshou Zhang - writing - original draft, experimental test & analysis; Jiang Ma - picture drawing & editing; Xizhen Ma – pre-experiment investigations & project equipment supply.

Conflict of interest: The authors state no conflict of

References

- Liu, Z., S. Cheng, and Q. Wang. Progress of boiler steel for [1] 600°C thermal power units in China, Metallurgical Industry Press, Beijing, 2011.
- Yang, S., Z. Liu, and S. Cheng. Performance analysis of key boiler steels for ultra-supercritical thermal power units. Journal of Iron and Steel Research, Vol. 22, 2010, pp. 37-56.
- Liu, Z. A steel for 650°C steam temperature ultra-supercritical thermal power unit and its preparation method, National Intellectual Property Office, China, 2014.
- Liu, Z. and X. Xie. The Chinese 700°C A-USC development program. Materials for ultra-supercritical and advanced ultrasupercritical power plants, Woodhead Publishing Ltd, Britain, 2017, 715-731.
- [5] Li, H., J. Liang, C. Zhou, and L. Xu. Effect of normalizing temperature on microstructure and room temperature strength of G115 steel. Metal Heat Treatment, Vol. 39, 2018, pp. 71-76.
- Xiao, B., L. Xu, L. Zhao, H. Jing, and Y. Han. Tensile mechanical [6] properties, constitutive equations and fracture mechanisms of a novel 9 % chromium tempered martensitic steel at elevated temperatures. Materials Science and Engineering: A, Vol. 690, 2017, pp. 104-119.
- Xu, L., H. Pang, and L. Zhao. Microstructure and mechanical properties of CMT + P welding process on G115 steel. Journal of Welding, Vol. 41, 2020, pp. 1-5.
- [8] Cai, H. Y., L. Y. Xu, L. Zhao, Y. D. Han, H. N. Pang, and W. Chen. Cold metal transfer plus pulse (CMT + P) welding of G115 steel: Mechanisms, microstructure, and mechanical properties. Materials Science and Engineering: A, Vol. 843, 2022, id. 143156.

- [9] Kumar, S., C. Pandey, and A. Goyal. A microstructural and mechanical behavior study of heterogeneous P91 welded joint. *International Journal of Pressure Vessels and Piping*, Vol. 185, 2020, id. 104128.
- [10] Kumar, S., C. Pandey, and A. Goyal. Effect of post-weld heat treatment and dissimilar filler metal composition on the microstructural developments, and mechanical properties of gas tungsten arc welded joint of P91 steel. *International Journal of Pressure Vessels and Piping*, Vol. 191, 2021, id. 104373.
- [11] Gaurav, D., S. Sachin, and P. Chandan. Study on microstructure and mechanical behavior relationship for laserwelded dissimilar joint of P92 martensitic and 304L austenitic steel. *International Journal of Pressure Vessels and Piping*, Vol. 196, 2022, id. 104629.
- [12] Chandan, P., M. M. Manas, K. Pradeep, and S. Nitin. Dissimilar joining of CSEF steels using autogenous tungsten-inert gas welding and gas tungsten arc welding and their effect on -ferrite evolution and mechanical properties. *Journal of Manufacturing Processes*, Vol. 31, 2018, pp. 247–259.

- [13] Chandan, P. Mechanical and metallurgical characterization of dissimilar P92/SS304 L welded joints under varying heat treatment regimes. *Metallurgical and Materials Transactions A*, Vol. 51A, No. 5, 2020, pp. 2127–2142.
- [14] T/CISA 003-2017. Seamless new martensitic heat-resistant steel tubes and pipes of 08Cr9W3Co3VNbCuBN (G115) for power station, 2017.
- [15] Liu, Z., Z. Chen, and H. Bao. Development and engineering of a new generation of martensitic heat-resistant steel G115, Metallurgical Industry Press, Beijing, China, 2020.
- [16] Abe, F. Precipitate design for creep strengthening of 9 % Cr tempered martensitic steel for USC power plant. Science and Technology of Advanced Materials, Vol. 9, 2008, pp. 1–15.
- [17] Abe, F. and S. Nakazawa. The effect of tungsten on creep. Metallurgical and Materials Transaction A, Vol. 23, 1992, pp. 3025–3034.
- [18] Yugai, S. S., L. M. Klediner, and A. A. Shatsov. Structural heredity in low-carbon martensitic steels. *Metal Science and Heat Treatment*, Vol. 46, 2004, pp. 539–544.